Special Issue
Seismology in India – An Overview

SEISMIC TOMOGRAPHY OF THE SOUTH INDIAN SHIELD

S. S. RAI, D. S. RAMESH, D. SRINAGESH, K. SURYAPRAKASAM, G. MOHAN, P. V. S. S. RAJAGOPALA SARMA and Y. SATYANARAYANA

National Geophysical Research Institute Hyderabad 500 007

and

V. K. GAUR

Dept. of Ocean Development, New Delhi-110 003.

ABSTRACT – *The South Indian shield, evolved through the accretion of several geologic units, provides a unique natural laboratory to explore and test the geodynamic hypotheses submitted to explain the origin and evolution of continents, nature of dissimilarity between continent and ocean, mountain building processes, intra-continental disruptions etc. Aiming at unfolding the mysteries of this vibrant geodynamic setup with an efficient geophysical explorer, a teleseismic depth sounding research program has been initiated at the NGRI that includes 3-D velocity tomography, imaging of lithospheric scatterers, shear wave splitting (anisotropy) and shear wave crustal modeling. Major results from this research initiative include:*

- *Presence of a thick upper mantle high velocity in large segment of the south Indian shield.*
- *Evidence for anomalous crustal thickening and low velocity in the uppermost upper mantle (till atleast 200 km) beneath the high grade terrain.*
- *Anomalous upper mantle low velocity signatures form the north west part of Deccan trap, Godavari rift and Kaladgi–Bhima Precambrian basins.*
- *Image of crustal topography in south India.*
- *Presence of dominant scatterers in lower crust/upper mantle beneath the Closepet granite.*
- *Near similar upper mantle anisotropy beneath Hyderabad and Poona seismological stations.*

INTRODUCTION

Geological framework of the south Indian shield is the cumulative effect of geodynamic sequences ranging from the early precambrian crustal evolution to the young volcanism over its north-west segment. Bounded in the north by the Narmada–Son lineament and Godavari rift system, major geological entities of south India (figure 1) include: the Dharwar craton–a granite-greenstone terrain; the southern granulite province–primarily a high-land, high grade terrain; the Eastern ghat granulite terrain (a granulite–Khondalite complex) and Deccan volcanic province. It also includes three intra-cratonic proterozoic basins: the Cuddapah–to the east of the Dharwar craton, Bhima and Kaladgi–seated between the DVP and Dharwar craton. The northern limit of Bhima and Kaladgi is unknown due to the Deccan volcanic covering over it. Dharwar itself has two subdivisions, east and the west, with the N-S elongated Closepet granite forming the hinge line between them. Except for the DVP (at 60–65 Ma) the other geological units have their ancestry from 0·15 to 3·4 billion years.

The detailed geology of the region is presented by Naqvi and Rogers[1]. Considering the wide distribution of geodynamic events in time and space it is imperative to believe that the south Indian shield has suffered multiple tectonic reworkings in the geological past. Whether such orogenies (young or old) have measurable geophysical imprints still left would essentially dictate our capability to decipher the nature of the past geological processes. Existing geophysical anomalies inherit their signature from the reminiscences of thermal, chemical or structural perturbation in the

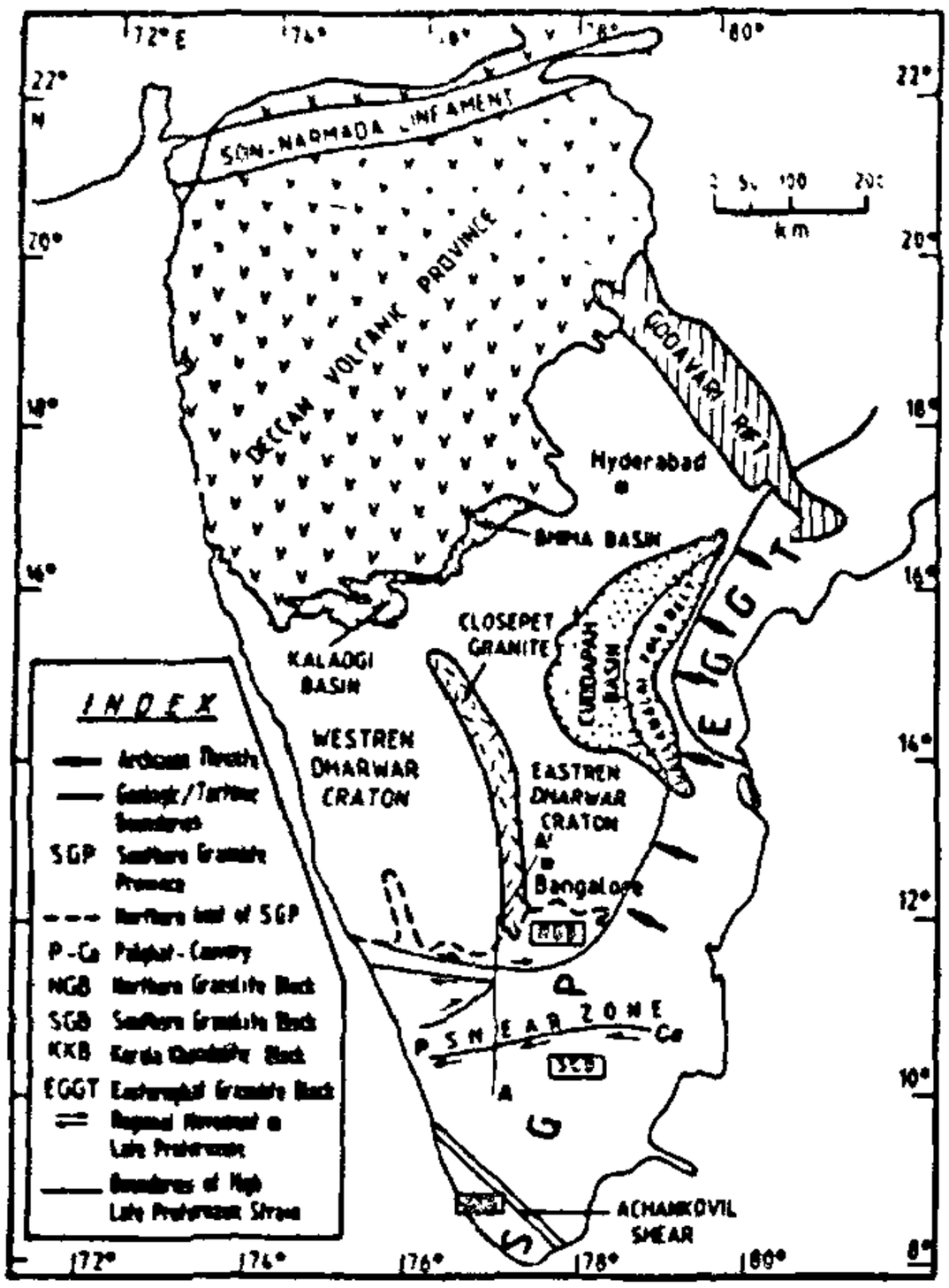

FIGURE 1 Geological framework of south India.

crust and upper mantle during orogenies. These perturbations led to changes in the material properties in the crust/mantle manifested in the geophysical signals (e.g. travel times of seismic waves).

Based on this premise an experiment to study the deep seismic characters of various geotectonic units in south India is being executed at the NGRI. The experiment uses earthquake waves to explore the lithosphere–asthenosphere system underneath the south India with the following major seismological components:

- 3-D Velocity tomography of south India,
- Imaging of seismic scatterers
- Study of seismic anisotropy and
- Shear-wave crustal modeling through waveform analysis.

3-D VELOCITY TOMOGRAPHY OF SOUTH INDIA

Travel Time Residual

The rays as they travel through the earth are either delayed or advanced relative to a homogeneous earth model depending on the nature of velocity inhomogeneities (slower or faster) encountered in their path. These delays or advancements (called 'residuals') provide a quantitative estimate of seismic heterogeneity. Residual is the difference between observed and computed travel time (for a spherical earth velocity model). For the j^{th} event and i^{th} station, the travel time residual can be written as:

$$R_{ij} = T^0_{ij} - T^{th}_{ij}$$

where T^0 is the observed travel time for the pair ij and T^{th} is the theoretical travel time based on the standard earth model[2,3]. The residual 'R' contains error due to origin time uncertainties, source mislocation, source and path inhomogeneities. In order to minimise these effects, relative residuals are computed with respect to an averaged residual. The relative residual for an event j recorded by N receivers is written as:

$$RR_{ij} = R_{ij} - 1/N \sum R_{ij}$$

The relative residual in the rest of this report would be referred to as 'residual'.

The residual averaged over the entire azimuthal range at a station reflects the nature of inhomogeneity vertically beneath the station. It is represented by:

$$AR_i = 1/M_i \sum_j RR_{ij}$$

where M_i events were recorded at station i. The averaged residual (also called 'Station anomaly') is independent of the event azimuth.

Data

We operated a number of temporary seismic stations (figure 2) in low and high grade terrain of south India. All the stations are equipped with 1Hz vertical seismometer and an analog portacorder operating at 240 mm/min speed. The stations were operated in a phased manner during 1986–87 and Nov. 89–Dec. 90. One cycle waveform of events for a number of stations are compared for consistency check. Generally the distinctive features of the waveforms like peak, trough, zero cross apart from the first arrivals (figure 3) are used to determine the travel time residual. Reading time accuracy is estimated to be around 0·05 secs. Travel time residuals are computed using Herrin's travel time table[2]. The average relative residual is computed by subtracting from each station residual, the average for all the stations recording the event. These residuals were corrected for the earth's ellipticity and the station elevation.

To the above travel time data sets we also added the

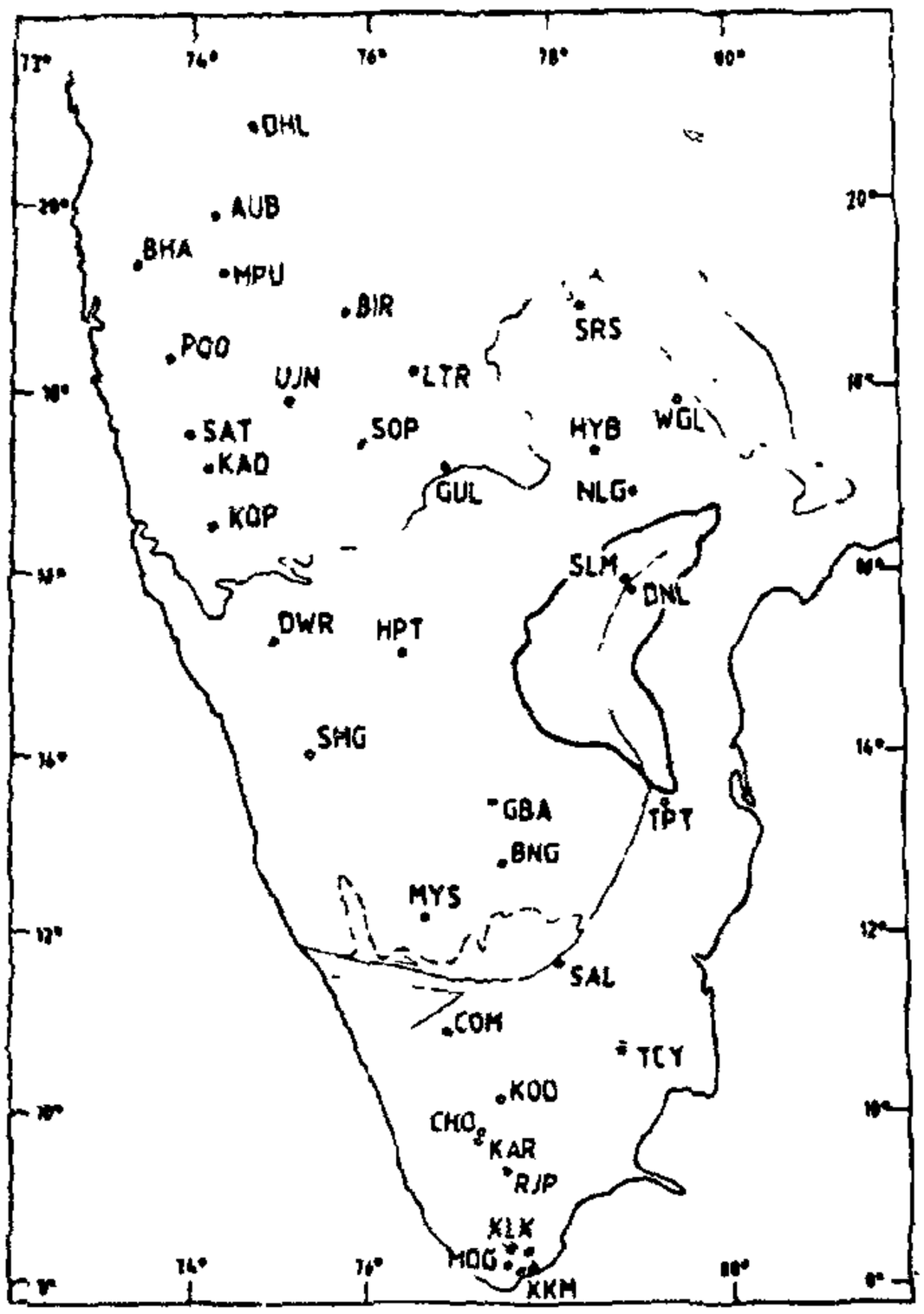

FIGURE 2 Location of seismic stations in different geotectonic terrains of S. India.

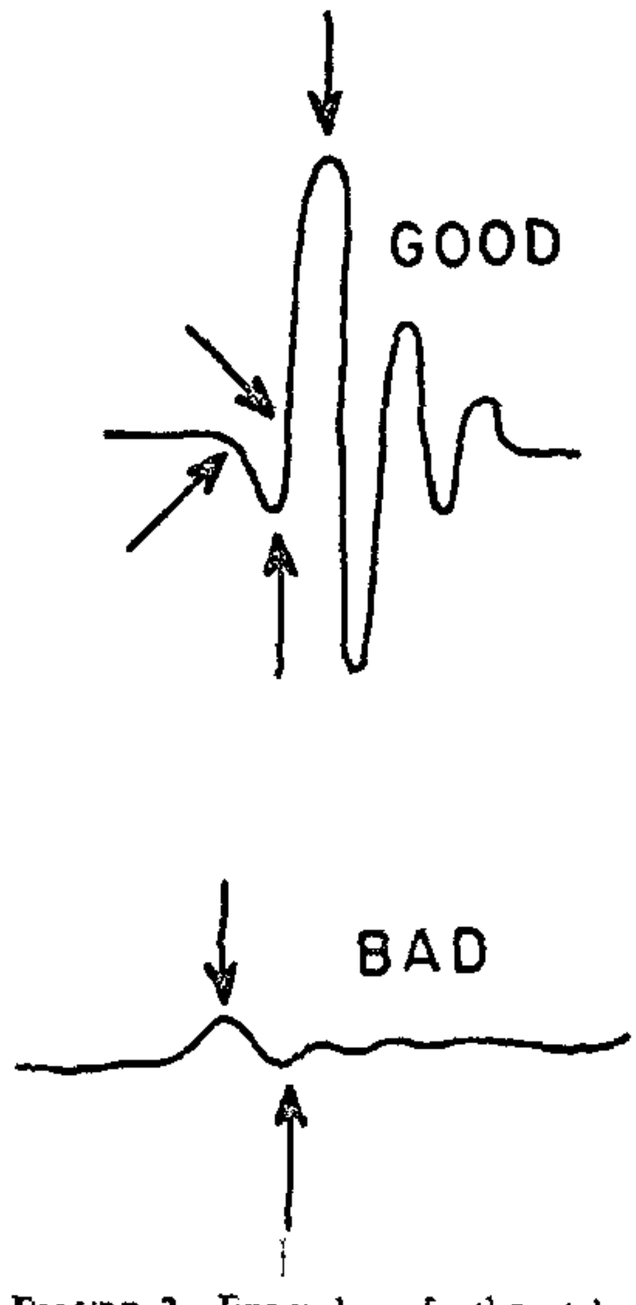

FIGURE 3 Example of the teleseismic signals. Arrow indicates the times used in the analysis.

observations from five most reliable permanent seismological observatories (HYB, POO, GBA, KAD, KOD) in south India. Travel times from earthquakes of magnitude > 5·5 with impulsive records were only considered. This data set comprised of over 1200 earthquakes for the period 1977–1986. To reduce the effect of reading error and the error in clock correction, residuals from the same source region ($2^0 \times 2^0$) were averaged. Of these five permanent stations three (HYB, POO, GBA) were also occupied by our temporary network. It is interesting to note that the source region averaged residuals from the permanent stations show almost a similar character as from our temporary stations.

Analysis of Travel Time Residuals

The interpretation of travel time residual is essentially based on analysis of its magnitude and spatial variation. The residual magnitude reflects the size of the anomalous zone, while the azimuthal variation is controlled by geometry of the inhomogeneity. An azimuth independent anomaly over considerable areal extent would be due to a relatively large deep seated target. Negative residual is a signature of high velocity, positive residual is due to low velocities and zero anomaly is an unknown reference velocity.

The residual at each station averaged over all the events ("station anomaly") primarily reflects the gross velocity variation under the station. Considering the large aperture of the array the station anomaly is a signature of the crust and the uppermost upper mantle. It defines the velocity configuration beneath the station till a depth level of 60–80 km, considering the common path of the ray for all the azimuthal ranges. In the present array the station anomaly is horizontally smoothened due to lateral inhomogeneity present within 30–40 km radius of the station.

Station anomaly for the south Indian stations is presented in figure 4(a). Primary features of station anomaly include: faster arrivals (station anomaly -0.05 to -0.33 secs.) of teleseisms over the granite-

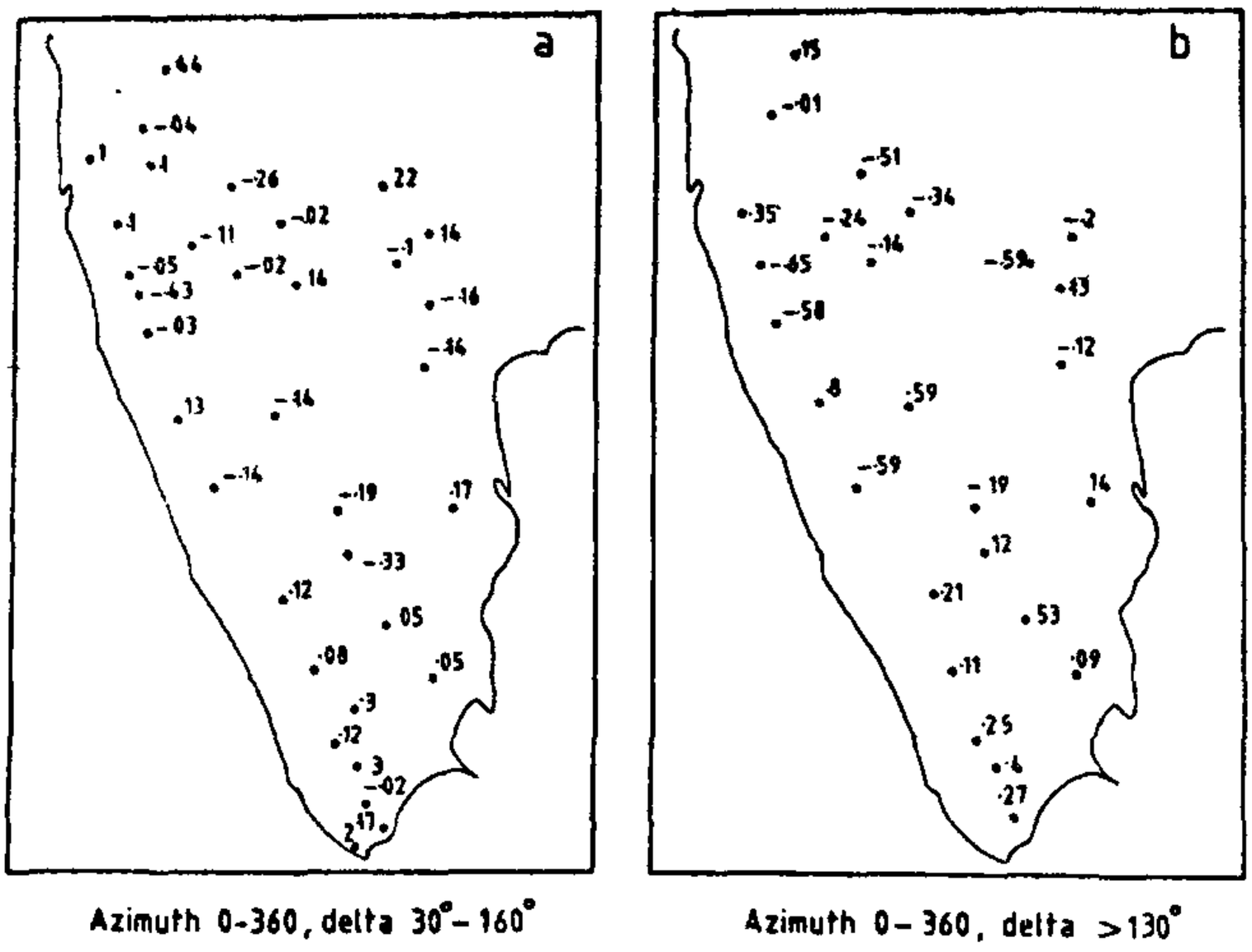

FIGURE 4(a) Average relative residual (in secs) independent of the azimuth ("Station anomaly"). Positive values indicate delay, negative indicate early arrival (azimuth 0–360°, delta 30–160°) (b) Average relative residual for PKIKP (azimuth 0–360°, delta >130°).

greenstone Dharwar craton; anomalous time delays (0·1 to 0·44 secs) in the north-west part of the DVP and a 0·05 to 0·2 secs of time delay over the highland high-grade terrain. The two major shear zones Palghat–Cauvery and Achankovil show significant intra-terrain teleseismic residual variations. These shear zones are approximately 0.2 to 0.4 secs faster than the rest of the granulite region. Compared to Palghat–Cauvery (station anomaly 0·05 to 0·08 sec for stations COM, SAL, TCY), the Achankovil shear zone shows faster arrival (− 0.02 sec). It is interesting to observe that to the north and south of these two shear zones the station anomalies do not show any evidence of seismic contrast, negating the possible continuation of shear zones at deeper level.

To observe the velocity character vertically beneath the station, the residual for PKIKP, (delta > 130°, incidence angle less than 6°) is plotted in figure 4(b). Being near vertical incidence, lateral variations have least effect on the PKIKP residuals. Except for very minor changes, PKIKP residuals exhibit similar character as the station anomaly. The only surprise is the positive residual at stations in the proximity of the Kaladgi–Bhima basins. It is important that the stations near the southern and eastern coast line also show delayed teleseismic response.

The residuals grouped according to the ray azimuths 0–90°, 90–180°, 180–270°, and 270–360° are presented in figures 5(a)–5(d) to examine the deep structural pattern of the causative source for travel time residuals in the southern Indian shield. At most of the stations residuals from different azimuths do not show any significant difference among themselves. The Dharwar craton is largely characterised by faster arrivals independent of the azimuth except at DWR, GUL and HPT. These stations are in close proximity to the Precambrian sedimentary basins, Kaladgi and Bhima where a large negative (upto − 110 mgal) Bouguer anomaly is also observed. The north-west DVP anomaly records time delay of 0.2 to 0.7 secs for all the azimuth events except those from the south-east. This restricts the source for the anomaly to continue to the central part of DVP. The stations SRS, WGL on the southern periphery of the precambrian Godavari rift show positive residuals (approx. 0.2 secs.) for northern and eastern events while those from south record faster arrivals (approx. −0.2 secs.). This contrast of 0·4 secs indicates significant low velocity in the upper mantle beneath the Godavari rift. In contrast to the regional faster arrivals in the low grade terrain, southern high grade terrain reflects delayed arrivals ranging from 0.05 to 0.5 secs. The azimuth independent signatures in both the terrains is a clear manifestation of very deep seated seismic structural dissimilarity beneath them. Source for such time delay could be crustal thickening and/or

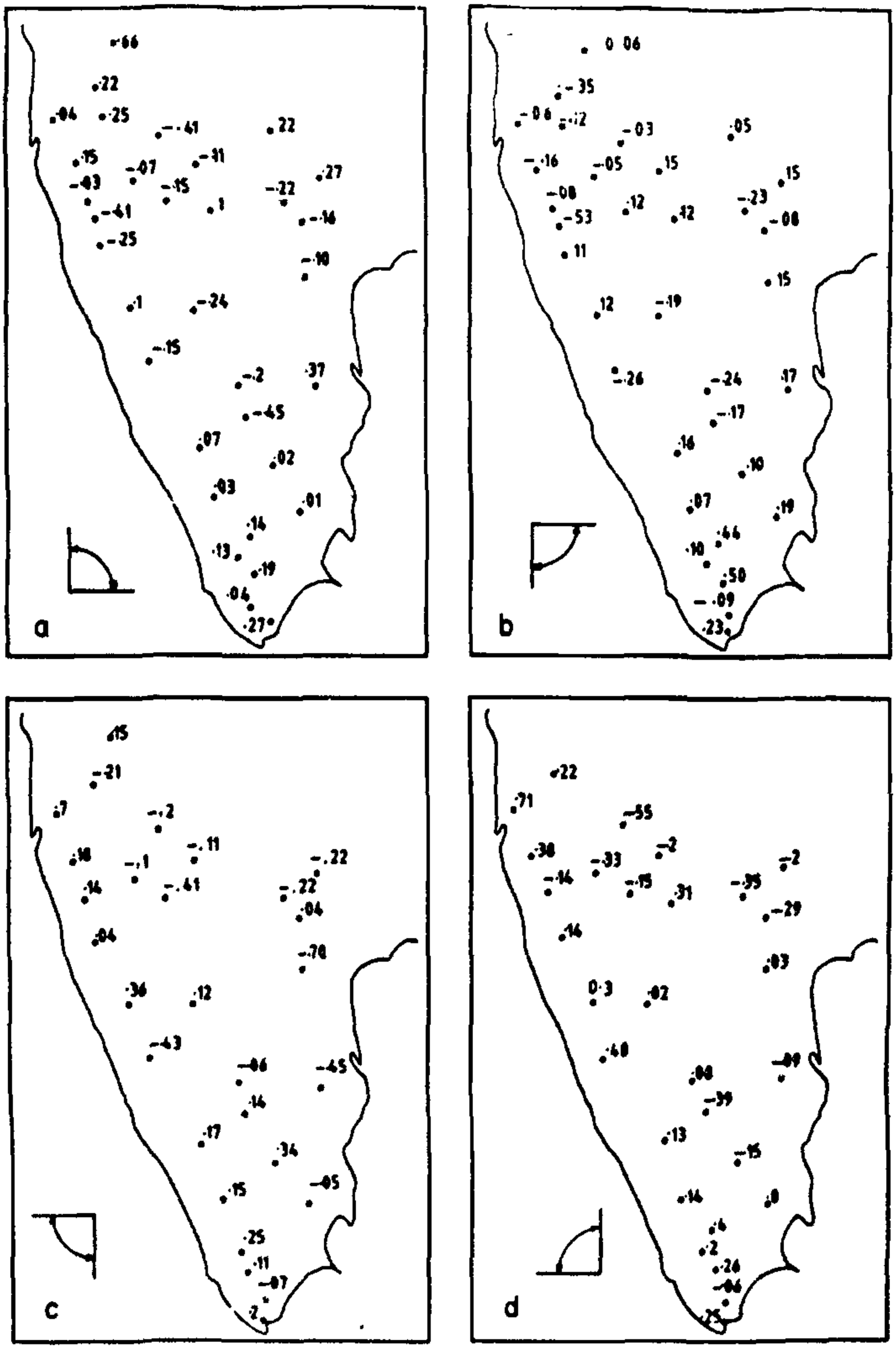

FIGURE 5 Average relative residuals for four major azimuth quadrants (a) 0–90 degrees (b) 90–180 degrees (c) 180–270 degrees (d) 270–360 degrees.

anomalous upper mantle. A thickened continental crust produces approximately 0.039 secs/km residual delay assuming an average crustal velocity of 6.4 km/sec and subcrustal velocity of 8.2 km/sec. The time delays of 0.4 to 1.0 secs observed in the Precambrian granulite terrain compared to the contiguous low grade Dharwar craton, is therefore difficult to be explained by the low velocity thickened crust alone and has partial contribu-

tion from the uppermost upper mantle also. This is also based on the observation that most of the granulite terrain stations show similar residual pattern implying that the lateral variations are not near surface effects.

The residual pattern though points to the dissimilar lithospheric character amongst the geologic units in south India, the lateral and vertical distribution of sources remains to be resolved. This we attempt to unfold through the 3-D travel time inversion of the residual amplitude and azimuthal behaviour.

Travel Time Inversion

Teleseismic imaging is a powerful tool to infer the crust-mantle structure (Aki *et al.*[4]; Ellsworth[5]; Taylor and Toksoz[6]; Hirahara[7]; Iyer[8]; Husebye *et al.*[9] and others). The "ACH" inversion technique[4] images the subsurface structure in terms of relative velocity perturbation from the basic data of relative residuals. The region of interest is divided into vertical layers and then gridded into rectangular blocks. Given an initial velocity model, the residuals are inverted in terms of the slowness perturbation in each block.

The basic equation governing the ACH inversion is

$$\gamma = Gm + \varepsilon$$

where γ is the relative residual vector, G the relative travel time path matrix, m the unknown velocity and ε the error term. The damped least squares solution to the above equation is:

$$\hat{m} = (G^t G + \theta^2 I)^{-1} G^t \gamma$$

$\hat{m}$ is the model estimate and θ^2 is damping parameter.

The solution $\hat{m}$ is the velocity perturbation in each block relative to an unknown velocity model. The absolute velocities cannot be determined here because the input data is relative rather than absolute residual. Choice of a velocity model helps only in the ray tracing and velocity variations upto 10% do not change the ray sampling pattern[6]. We used the velocity from the Herrin's velocity model[3] for spherical earth with crustal velocities replaced by DSS modeling results in the area[10]. The velocity perturbation in each block is however independent of choice of the velocity model. The block size is controlled by the station spacing. The minimum number of rays sampling each block is fixed at 10. Due to the uneven station distribution with 100–150 km separation, the horizontal block size was kept 150 × 150 km. In the depth the inversion was carried out upto 600 kms. To ensure that the obtained anomaly patterns are not an artefact of adhoc block placement, blocks were shifted by half block width and rotated in several directions. The changes in the anomaly patterns thus obtained were insignificant. Due to uneven and large station separation in the region, decoupling the crustal effect from the uppermost upper mantle is not an easy task and no single model would alone be able to provide a reasonable solution to the geologic problems in south India. It is important to note here that any tomography result is basically model dependent. To have adequate sampling and resolution a relatively thicker surface layer was assumed. Details of the model is presented in table 1. This model serves the basic objective of quantifying the broad nature of crust/mantle dissimilarity between the terrains and provides the first signature of deep seismic structural character of the region. The velocity anomaly for S. India at various depth levels is presented in figure 6.

The velocity perturbation till 60 km is essentially controlled by the crust and uppermost upper mantle signatures. North west part of the DVP has large low velocity (− 4 to − 5%) whereas to the east of DVP in peninsular gneiss a contrasting high velocity (0·3 to 1%) is recorded. The southern granulite terrain is marked by significant low velocity (−2 to −6%) in the depth range of 0–60 km in contrast to the − 0·6 to − 0·2% low velocity in the low grade terrain. There is a progressive increase in the low velocity anomaly of high grade terrain from north to south except for the region coinciding with the Palghat–Cauvery shear zone and Kerala Khondalite block. The velocity distribution in the depth range of 0–60 km has contribution from the crust and uppermost upper mantle. One possible reason for this low velocity could be anomalous crustal thickening. However, if thickening is the only source for the low velocity it is unlikely that the velocity reduction pattern from north to south in the granulite will be reflected in the deeper layers into the upper mantle. To further resolve the depth level of dissimilarity between various terrains we examine the velocity configuration in the depth range 60–300 km.

In the depth range of 60–300 km, south India, on average, is characterised by high velocity upto + 1.4% with significant magnitude variation in different geologic blocks. The faster velocity (+ 1.2 to 1.4%) observed over the Dharwar craton is a reflection of it being the most stable and oldest geologic unit in south India. Presence of such thick high velocity upper mantle is best explained in the context of lithospheric roots or tectosphere[11,12] beneath the southern Indian shield.

TABLE 1 Initial Model for 3-D Block Inversion of South India Travel Time Residual Data

Layer	Thickness (km)	Horizontal Size (km)	Velocity (km/sec)
1.	60	150 × 150	6.78
2.	240	150 × 150	8.55
3.	300	150 × 150	10.09

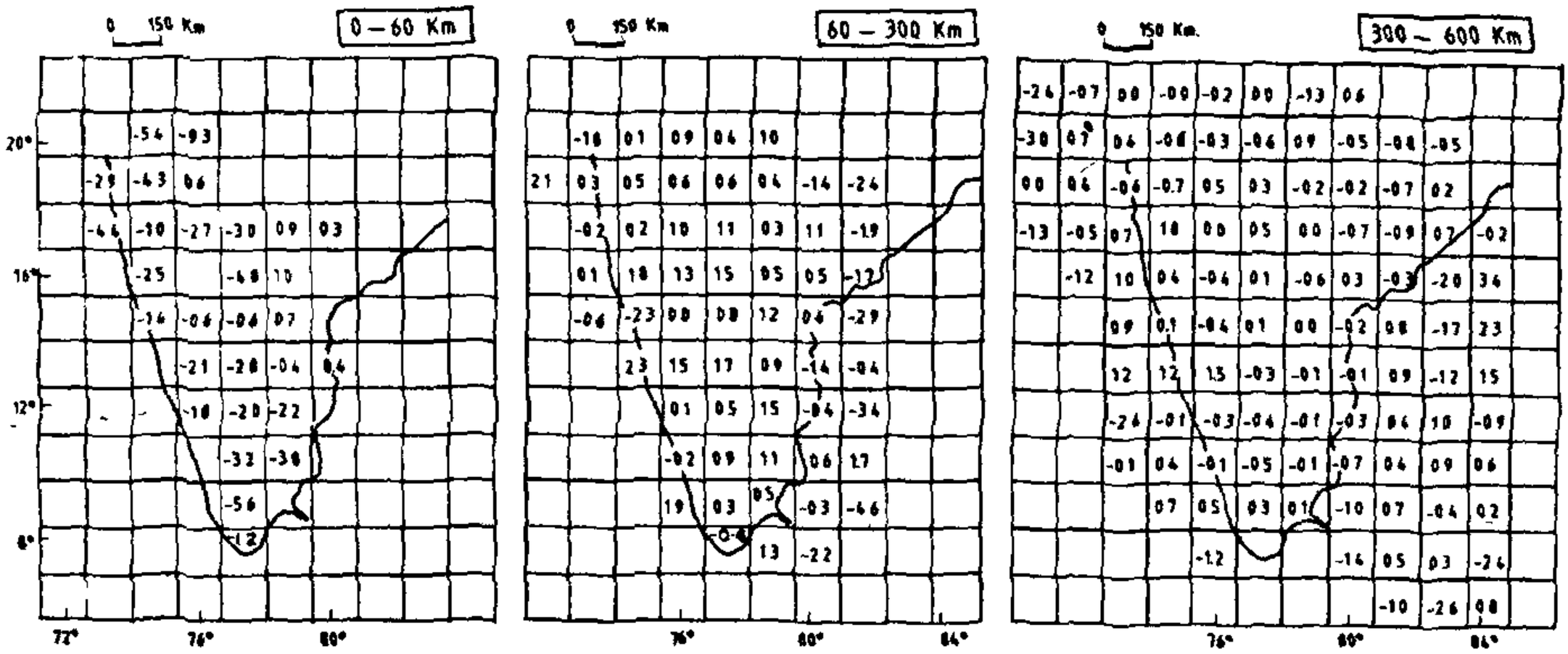

FIGURE 6 Velocity anomaly in south India at various depth levels.

With Dharwar (+ 1.2%) as the reference a progressive southward velocity decrease (+ 0.2 to 0.4%) is observed in the granulite terrain. Further south, Kerala Khondalite block shows anomalous low velocity (− 0·8%). Thus the granulite terrain is characterised by 1 to 2% low velocity compared to the Dharwar craton in the depth range of 60–300 km. The low velocity observed in 0–60 km below the granulite terrain, therefore, continues even beyond 60 km depth. It is interesting to observe significant low velocity also along the easternghat granulite terrain (EGGT). However, due to sparsity of seismic stations along the EGGT we shall refrain from making any geological correlation of the observed low velocity below this terrain. The results also indicate two major low velocity zones coinciding with the Godavari rift (− 1.4 to − 2.4%) and Precambrian Kaladgi–Bhima basins (0.0 to 0.8%).

Velocity tomography in the depth range of 300–600 kms do not show any coherency with the layers above it. Also the associated error for most of the blocks are very high. In view of this we do not give any credence to these numbers.

THE CRUST BENEATH SOUTH INDIA

Crust being the end product of any tectono-thermal event, occupies a pivotal place in studying the tectonic history of the region and therefore defining its basic configuration in terms of the velocity and thickness is the most basic information needed in any geodynamical investigation. Unfortunately, even this is not available for most of the south Indian terrains. We attempt to fill this gap through the teleseismic tomography.

Application of teleseismic tomography to study the crustal character involves computing the velocity perturbation beneath each station while the subcrustal zones are modeled with rectangular blocks. The details of the model is presented in table 2. We choose horizontal dimension of the block to be one degree on a side. Using this model we attempt to compute the crustal thickness and velocity parameters. Assuming a homogeneous crust, Iyer and Healy[13] computed the crustal thickness from the station anomaly over the LASA. Though the assumption of a homogeneous crust is valid for LASA, combination of Precambrian orogenic belts in the modeling region of south India necessitates combining velocity variation and station anomaly together to compute crustal thickness.

The method has been successfully applied in a similar geologic scenario in NE United States[6]. It is based on the assumption that the crustal velocity perturbation $\delta V/V$ is fluctuation from a reference crustal velocity V_c. The average crustal velocity beneath a station i is therefore,

$$V_i \simeq V_c[1+(\delta V/V)_i/100],$$

and the crustal thickness is

$$h_i \simeq V_i R_i + h_0,$$

TABLE 2 Initial Velocity Model for Computation of Crustal Parameters

Layer	Thickness (km)	Horizontal Size (deg)	Velocity (km sec)
1.	35	1 Block/Station	6.53
2.	215	1 × 1	8.38
3.	250	1 × 1	9.58

where h_0 is the assumed average crustal thickness and R_i is the station anomaly. It may be recalled again that during the inversion information related to absolute velocity is lost and therefore the crustal parameter computed as above are only first order approximations to the reality. All the input data was corrected to the MSL. Average crustal velocity was assumed as 6·5 km sec for 35 km thick crust. The resulting crustal thickness and velocity maps are shown in figure 7. The crustal thickness was found to be influenced more by the station anomaly and the choice of initial crustal thickness did not change the final crustal thickness. Crustal thickness (d) and velocity (v) varies between 34–39 km and 6·0–6·6 km/sec beneath south India with an average of 35 ± 1 km and 6·5 ± ·1 km/sec in most parts of the region. Deviation from this is observed in the southern granulite terrain (d = 36–38 km, v = 6·3–6·5 km/sec), north west part of DVP (d = 37–39 km, v = 6·0–6·1 km/sec) and the region bordering Proterozoic basins (d = 37 km). The most noticeable crustal thinning of 3 km exists beneath the Karad bounded on its north and south by 36 km thick crust. Anomalous low velocity crust (6·0–6·2 km/sec) characterises the north west and the south west part of DVP. While the former one coincides with the Deccan basalts source region the latter one is on the fringes of the Precambrian sedimentary basins. Further refinement of crustal thickness and velocity presented here is in progress.

TOMOGRAPHY OF LITHOSPHERIC SCATTERERS

A seismic wave travelling in a heterogeneous medium is scattered when it crosses an inhomogeneity comparable to its wavelength. The incident power is then scattered in different azimuths with large angles to the incident direction. The scattered energy is recorded at the surface of the earth as coda waves[14,15]. For local earthquakes, coda waves constitute the end portion of the seismogram whereas at greater distances they are recorded as P coda and lie between the direct P and S phases. Scattering studies have been conducted based on coda analysis by Aki[16], Wu & Aki[17] and several others. Excellent reviews on the subject are presented by Herraiz and Espinosa[15] and Wu and Aki[17]. Array data also makes it possible to follow the scattered waves across the array, thus obtaining the time shifts which can be utilized to delineate the zone of dominant scattering[18,19]. We image the lithospheric scatterers in the Precambrian shield of south India by applying the technique of semblance on GBA array data.

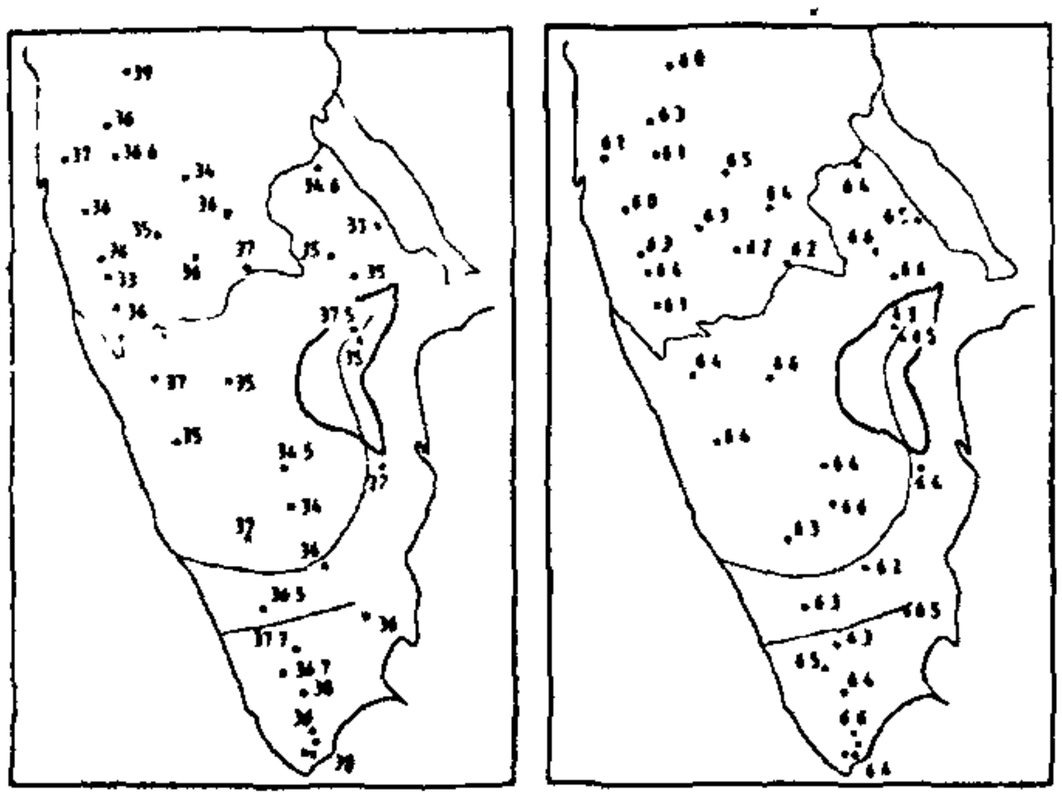

FIGURE 7 Crustal thickness and velocity map of south India.

GBA Array and General Geology

The Gauribidanur (GBA) seismic array situated about 60 km north of Bangalore in south India provides an excellent opportunity to investigate the inhomogeneities present beneath the array. GBA is situated on the western flank of the eastern Dharwar Craton, the oldest geologic province (3·4 byrs.) in south India (figure 8). The array is close to the potassium rich N–S extending Closepet granite intrusion ~ 20 km wide and ~ 500 km long probably of lower crust/mantle origin[20]. Swaminath *et al.*[21] proposed that this long granitic intrusion is a suture-line between the western and eastern Dharwar craton. The GBA array is an L shaped array consisting of two orthogonal arms, the red and the blue (figure 8). The array consists of twenty short period (1 Sec) vertical component seismometers placed ten on each arm with a spacing of 2·5 km. The GBA array lies in a relatively flat lying area and the topographic contribution to the scattering is therefore minimal. The signals detected by the array are passed through a high cut filter of 7*Hz* prior to being recorded on magnetic tapes in digital form with a sampling interval of 0·05 sec.

Using the local earthquake data Arora[22] proposed a two layer crustal model of thickness 16 and 19 kms with the corresponding P-wave velocity of 5·7, 6·5 and 8·0 km/sec beneath the GBA seismic array. Berteussen *et al*[23] inferred an exceptionally homogeneous crust/mantle structure beneath the GBA array through a statistical analysis of teleseismic travel times across the array using Chernov's theory[24].

Data

Twenty six earthquakes from different depths and azimuths have been considered for this study (table 3). The three major azimuths of 340–350°, 45–65° and 100–115° correspond to the Afghan–Hindukush, China–

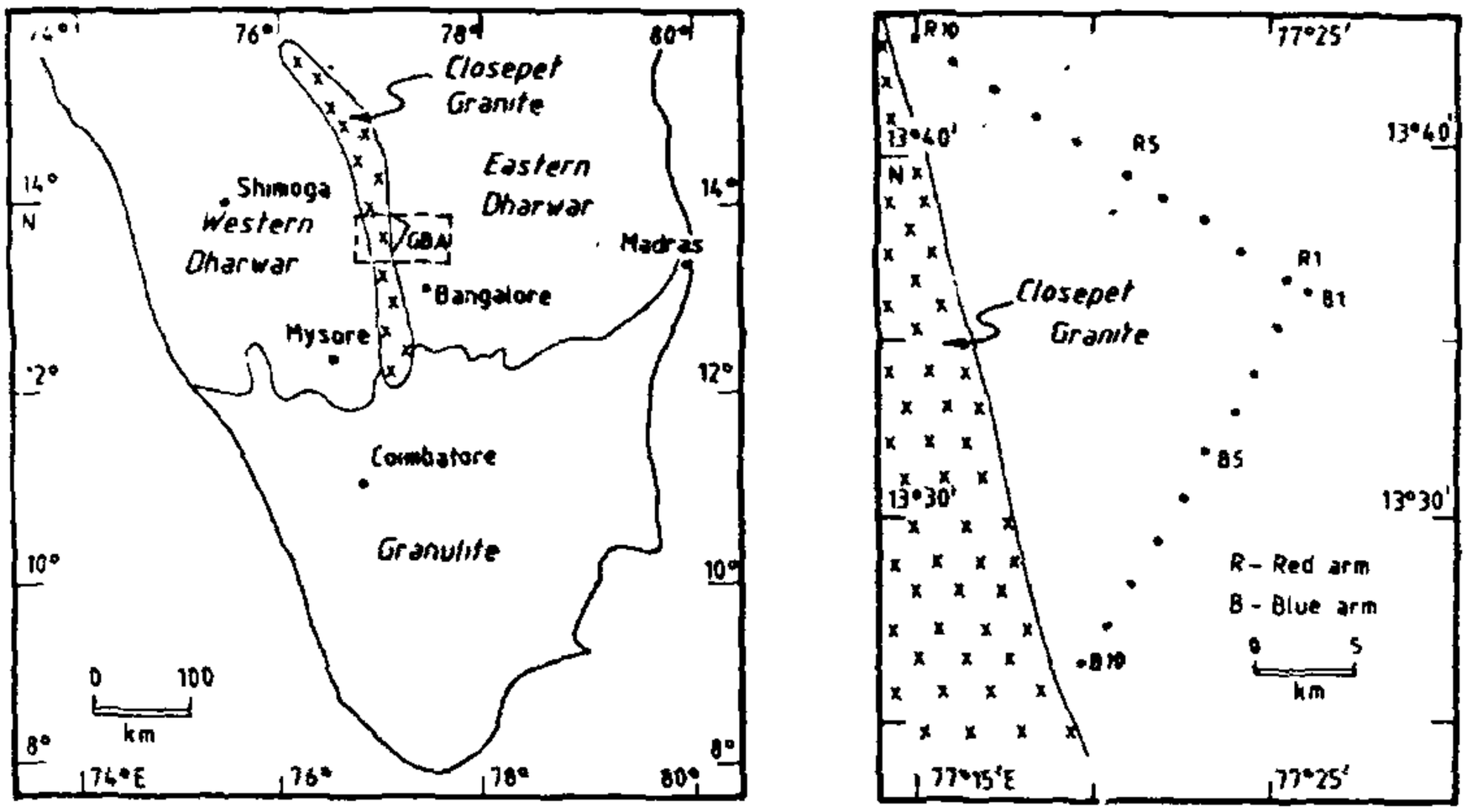

FIGURE 8 Location map of GBA seismic array.

TABLE 3 List of Events used in Scattering Studies

No.	Event	Date	Time	Lat + °N − °S	Long E	Depth Kms	Dist Δ°	Azm °	Group
1.	Afussr	01/10/81	13 14 50.8	36.42	71.47	122	23.34	347.78	I
2.	Echina	02/01/81	15 39 46.9	29.28	128.1	229	49.29	64.04	II
3.	Tadkhist	03/07/81	12 24 01.1	38.08	72.72	116	24.73	351.07	I
4.	Burma	04/25/81	11 32 23.0	24.90	95.34	146	20.26	53.68	II
5.	Hindkush	04/28/81	17 54 16 3	36.42	70.95	189	23.45	346.76	I
6.	Hindkush	11/01/81	09 22 37.0	36.46	70.72	202	23.54	346.34	I
7.	Eruschin	11/27/81	17 21 44.3	42.93	131.19	525	54.48	46.69	II
8.	Nsumtera	03/07/82	14 08 15.2	03.83	97.45	127	22.01	114.36	III
9.	Afghan	09/12/82	15 42 08.3	36.52	71.10	205	23.51	347.12	I
10.	Usrchina	10/08/83	07 45 26.3	44.21	130 74	551	54.53	45.07	II
11.	Hindkush	12/30/83	23 52 39.5	36.42	70.75	209	23.43	345.60	I
12.	Hindkush	01/02/84	00 39 35.8	36.46	70.72	202	23.54	346.34	I
13.	Hindkush	02/24/84	12 51 29.9	36.45	70.86	213	23.50	346.60	I
14.	Echina	04/15/84	07 34 11.1	42.87	131.20	528	54.47	46.77	II
15.	Hindkush	04/19/84	02 53 12.5	36.47	70.90	198	23.51	346.71	I
16.	Hindkush	08/22/84	18 00 53.4	36.10	70.53	131	23.24	345.71	I
17.	Hindkush	07/29/85	07 54 44.5	36.21	70.90	102	23.26	346.51	I
18.	Afussr	07/29/85	12 42 41.1	36.34	71.29	117	23.30	347.37	I
19.	Afghan	01/14/86	03 03 37.3	36.37	71.02	241	23.39	346 86	I
20.	Nicobar	06/02/86	17 51 56.1	09.12	93.51	93	16.37	104.16	III
21.	Hindkush	05/05/87	15 40 47.5	36.27	70.41	211	23.43	345.60	I
22.	Shonshu	12/01/89	04 57 18.7	30.80	137.14	492	57.24	62.01	II
23.	Vanuatu	12/01/89	18 59 09.1	− 14.41	167.35	189	93.23	103.97	III
24.	Koyna	10/21/85	11 38 10.0	20.70	72 60	10	8.51	340 00	I
25.	Koyna	10/21/85	14 30 50.0	20.70	72.60	10	8.54	340 00	I
26.	Valsad	06/13/86	01 26 15.0	21.20	73.15	9	9.65	341 00	I

USSR and Nicobar–Vanuatu regions. To avoid earthquake source region complexities deeper sources were selected for the study. Local events from Koyna and Valsad which are to the NW of GBA have also been taken into consideration. The earthquakes are classified into 3 groups according to their azimuths as shown in table 3. The digital data of one minute duration corresponding to the P coda is used in this analysis. We

observed from the frequency spectrum that the majority of the signal falls between 0·5–2Hz with peak amplitude at 1Hz.

The seismograms of some of the events used in this study are shown in figures 9(a–d). A progressive decrease in the scattered energy with increasing source–receiver distance is evident from seismograms in figure 9. Also the coda decreases significantly with increasing source depth (figure 9a and 9c). Similar observations have also been made by Kennett[25]. A local event shown in figure 9d from Koyna, about 800 km NW of GBA shows dominant scattering from the local heterogeneities.

Semblance Technique and Imaging Method

Semblance quantifies the coherency observed in the seismic traces recorded for an event[26] and is defined as the ratio of the total energy obtained from a cumulative stack of traces to the sum of the individual energies of each trace. The semblance ratio at a point in space is given by:

$$S_{x,y,z} = \sum_j \left\{ \sum_{i=1}^{N} h_i A_{i,j+x(i)} \right\}^2 \Big/ N \sum_j \left\{ \sum_{i=1}^{N} h_i A^2_{i,j+x(i)} \right\}$$

where N = number of channels

$x(i)$ = Time shifts for the ith channel

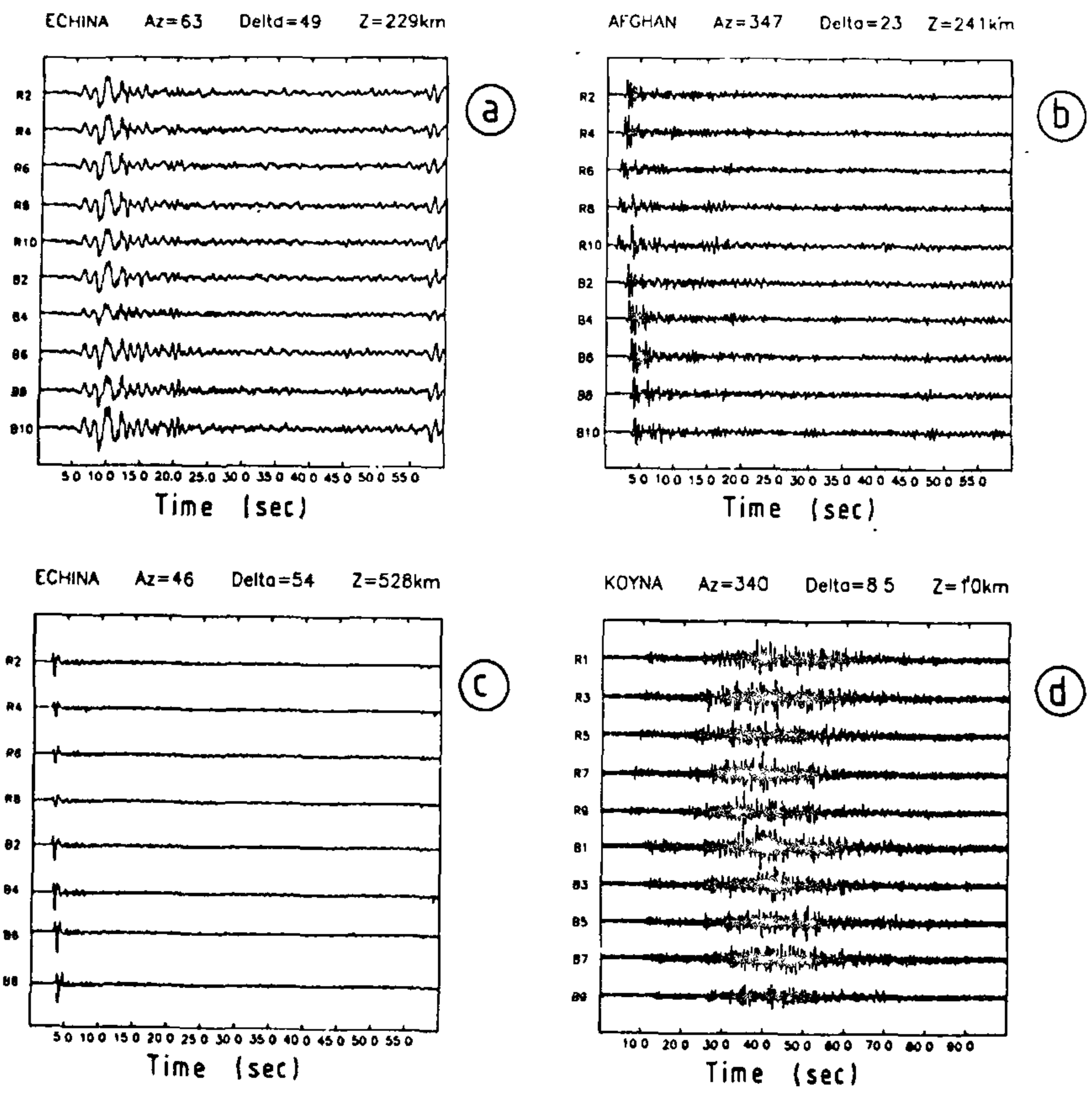

FIGURE 9(a–d) Seismograms of teleseismic and regional events 2 (29.28 N, 128.1 E), 19 (36.37 N, 71.02 E), 14 (42.87 N, 131.20 E) and 24 (20.70 N, 72.60 E) (table 3).

j = Time interval for stacking
$A_{i,j+x(i)}$ = Amplitude at time $j+x(i)$ in the ith channel
h = weighting factor which takes a value of 0 to 1.

The S ratio has a maximum value of 1 when there is complete coherency between all the seismic traces. It would be physically impossible to obtain this value in the real earth. As the earth is highly heterogeneous it is possible to obtain relatively high semblance values as compared to the background in certain regions which points towards a possible zone of dominant scattering.

The imaging method assumes a rectangular grid of points below the array at different depths. Grid points are equidistant and separation between them increases with depth giving the grid a conical shape. The coordinate of grid point 1 (figures 10–12) is 13·143° N, 77·234° E with 11 points on the X-axis pointing towards East and 19 points along Y-axis pointing North. Every point on the grid is assumed to be an isotropic point scatterer radiating energy which is received at the surface by an array of seismometers. Assuming a layered earth model the travel times required for the scattered rays from a point to reach the array are calculated. The crustal velocity model beneath GBA is adopted from Arora[22]. The minimum travel time observed at the receiver in the array serves as reference and is subtracted from travel times computed for all the channels. This gives the time delay $x(i)$, where i is the channel number, subtended at each receiver by a scatterer. The time delay at the receiver closest to a scatterer is zero. The traces from all channels are then stacked over a time window starting a few seconds after the P onset to exclude the high energy of the P wave. The energy in the stacked signal and summed energy from individual channels is then calculated. The ratio of these two energies gives the S ratio at a particular grid point. Similarly the S ratios at all the grid points in a layer are calculated and the procedure repeated for all the layers. The spatial distribution of the high semblance values indicates a possible zone of scattering. The methodology is similar to that presented by Lay[18], Lynnes & Lay[27]. A major hurdle in delineating the zone of scattering is the source effect[16,27] which swamps the energy radiated by scatterers. This is due to high energy of the source which introduces a focusing effect and needs to be eliminated.

To extract the source effect in the seismogram we follow the procedure involving delay and stack or beam forming[28] of seismograms from the array. This includes: picking the arrival times at the channels, computing their time shifts with respect to the earliest arrival time channel and stacking the seismogram with these time shifts. The stacked trace is an average over the number of channels, and represents the effect largely due to the source. This is then removed from each trace yielding a set of seismograms free of the source effect. The semblance technique is then applied to this filtered data set.

RESULTS AND DISCUSSION

To demonstrate the effectiveness of source effect filtering method presented above, the S plots for event 19 is presented in depth range of 5–55 km (figure 10). Note that in figures 10–12 the grid spacing is 2 km for the first 5 km depth and increases by 0·5 km for each depth increment of 10 km. The filtering effect is clearly visible in figures 10(a–b) with the semblance value at the same depth levels, before and after filtering. Figure 10 is for event 19 from Afghan with a NW azimuth (347°) from receiver to the source. Figure 10a (includes source effect) shows a clear tendency of the high semblance values to migrate with depth in the NW direction whereas figure 10b (filtered for the source effect) does not exhibit such a pattern. The plots in figure 10b show large scattering effect with the dominant scattering apparently around coordinates corresponding to the region 15–20 km west of cross point of the array. The scatterer is prominent in the deep crustal and uppermost upper mantle level (30–55 km). Similar observations are made from figure 11a & 11b which are from event 14 (azimuth 46°) and event 23 (azimuth 103°). In both figures the increasing semblance is not correlated with the ray direction. Beneath the array no significant scattering zone is observed. This is in conformity with the conclusions of Berteussen *et al.*[23].

To add credence to this conclusion the events from an azimuth group (table 3) are summed to yield an average S ratio plot for different depth levels. These averaged S plots calculated for azimuthal windows 340°–350°, 45°–65° and 100°–115° are shown in figure 12(a–c). The pattern does not change significantly as compared to the S plots of the three single events shown in figures 10b, 11a and 11b. The maximum semblance is observed over a 15 km × 15 km area with centre at 13° 35·5' N, 77° 14' E. This zone of scattering to the west of the GBA array cross point coincides with a zone of geologic contact (figure 8) between the east and west Dharwar craton and is often referred as a suture between the two cratonic blocks[21]. The deep crustal/upper mantle continuity of this scattering zone is also supported from the anomalous time delays for teleseisms crossing the Closepet granite[29] and recorded over the GBA array.

We analysed and modelled the coda waveforms from regional and teleseismic events recorded at Gauribidanur (GBA) seismic array in the Precambrian shield of south India to image the seismic scatterers using semblance

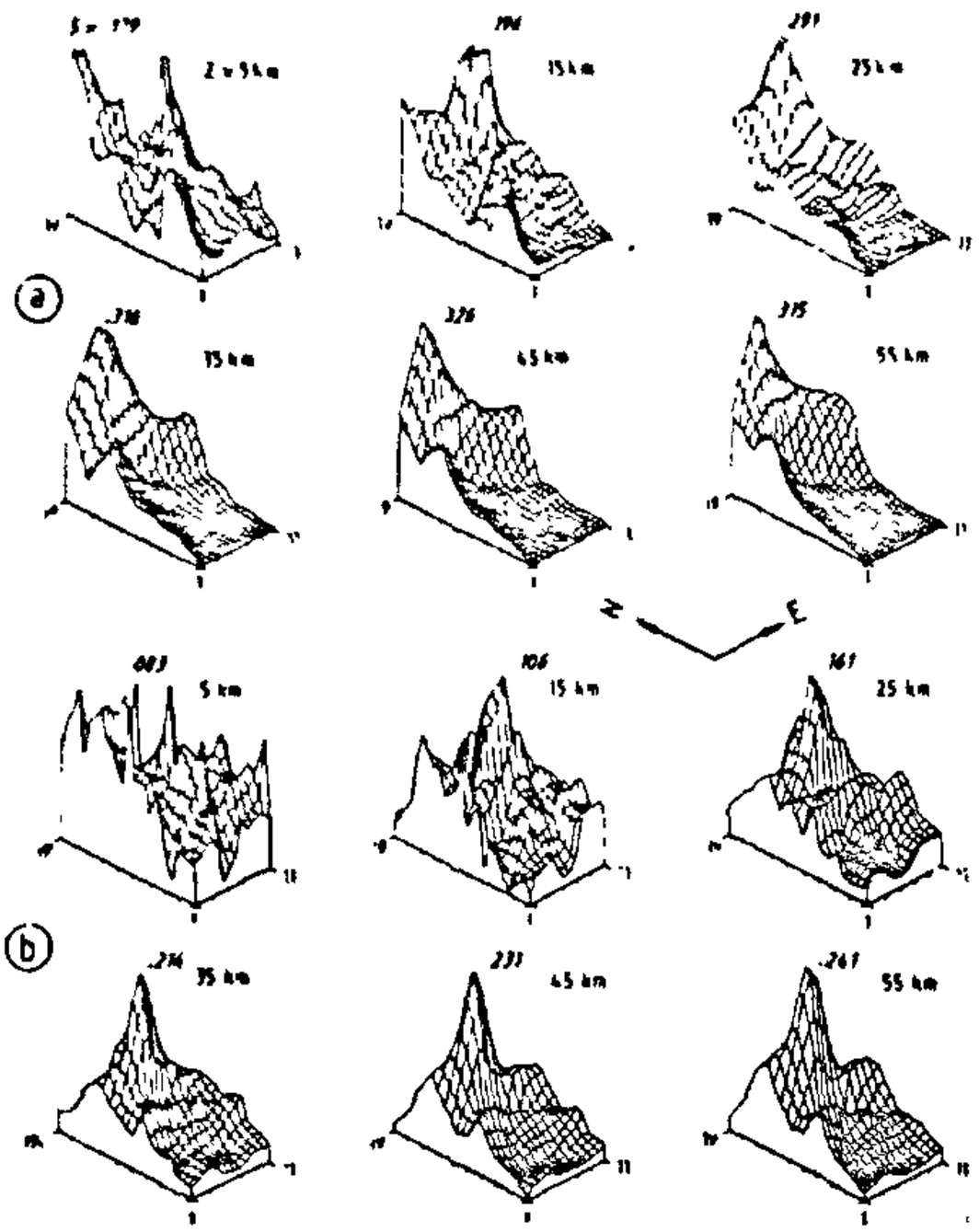

FIGURE 10(a–b) Semblance plot for event 19 at depth levels from 5 to 55 kms using (a) data not filtered for the source and (b) data filtered for the source effects. Note the absence of depth dependent semblance directivity in (b) as observed in (a). Coordinate for point 1 in the grid is 13.143 N, 77.234 E. Grid spacing is 2 km for the first 5 km and increases by *0.50 km for each depth increase of 10 kms.*

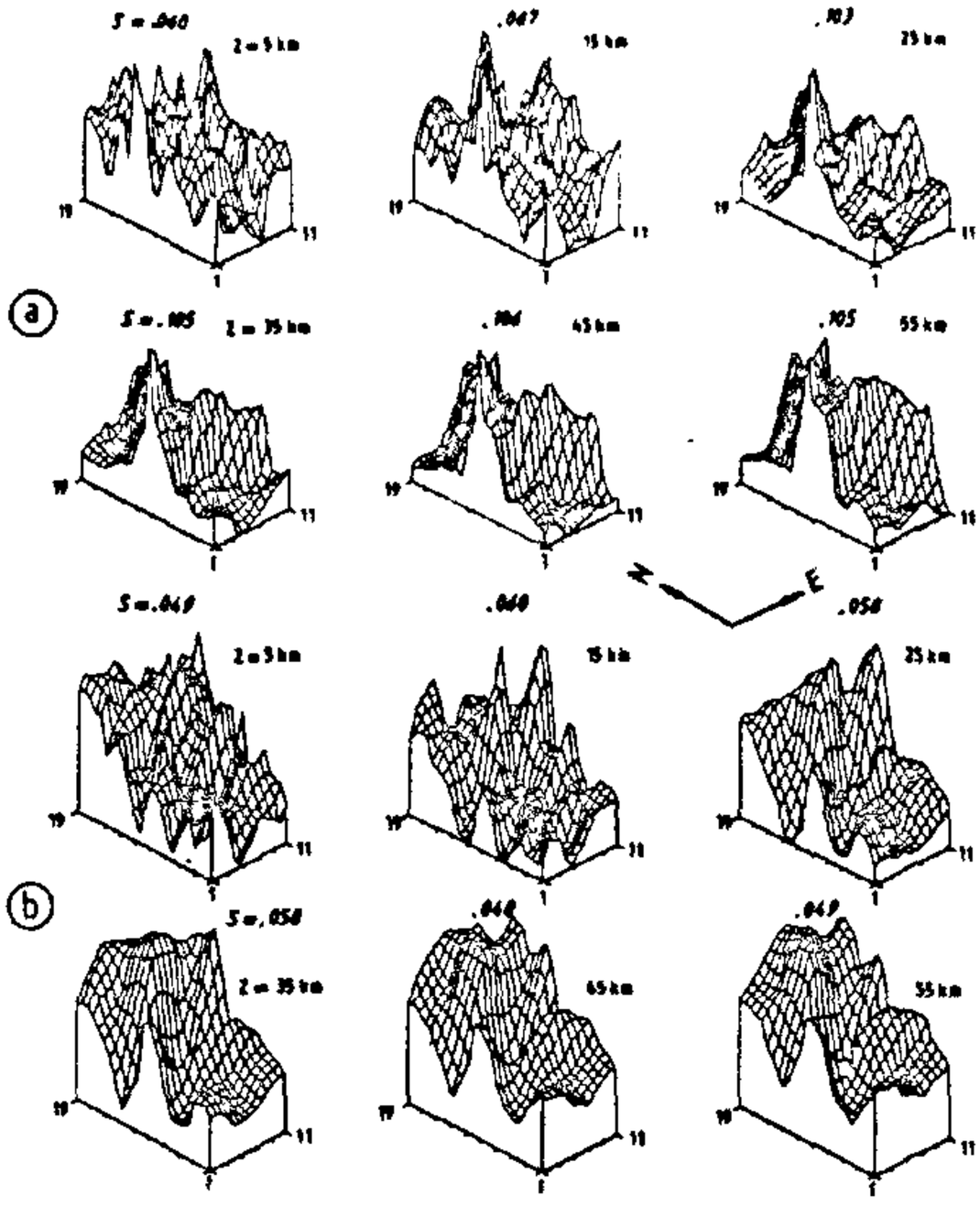

FIGURE 11(a–b) Source effect filtered semblance plot at depth level (5–55 km) for events 14 and 23. Grid specifications as in figure 10.

technique. High semblance values are observed at deep crustal and uppermost upper mantle level to the west of the array coinciding with a major geologic contact between two Precambrian cratons. The contact zone is an elongated granitic intrusion which originates from upper mantle material. The result is in agreement with the complex geological processes at the early history of evolution of Dharwar craton. The study shows the potential of the seismic scattering tomography technique in imaging geologic contacts.

SEISMIC ANISOTROPY IN SOUTH INDIA

Seismic anisotropy in the lithosphere is usually the reflection of a coherent trend of highly anisotropic crystal systems that get preferentially aligned along the flow direction during rock deformation. This, in turn, is determined by the shear history in a convective mantle revealed by its various signatures, notably, the azimuthal variation of P and shear wave velocities and polarization of shear waves. Seismic anisotropy is thus becoming an important diagnostic tool in deciphering the structure, composition and dynamics of the earth's interior. The existence of seismic anisotropy in continental structures is best manifested by the phenomenon of shear wave splitting observed in the low frequency range. The SKS waves from distant earthquakes that traverse the entire mantle as an S-wave along a nearly vertical path and the outer core as a P-wave, provide excellent lateral resolution and emerge as the best possible candidate for probing continental anisotropy. In a laterally homogeneous and isotropic medium therefore, these SKS waves will be polarized in the vertical plane of propagation as SV-waves, thereby, greatly limiting the energy carried by the transverse component (T-component). The characteristic properties[30] of azimuthal anisotropy are:

- The T-component of SKS is shifted in time with respect to the radial (R) component by a quarter period.
- The amplitude ratio T/R has an angular period 180° i.e. the T component of SKS behaves in time like the derivative of the R component.

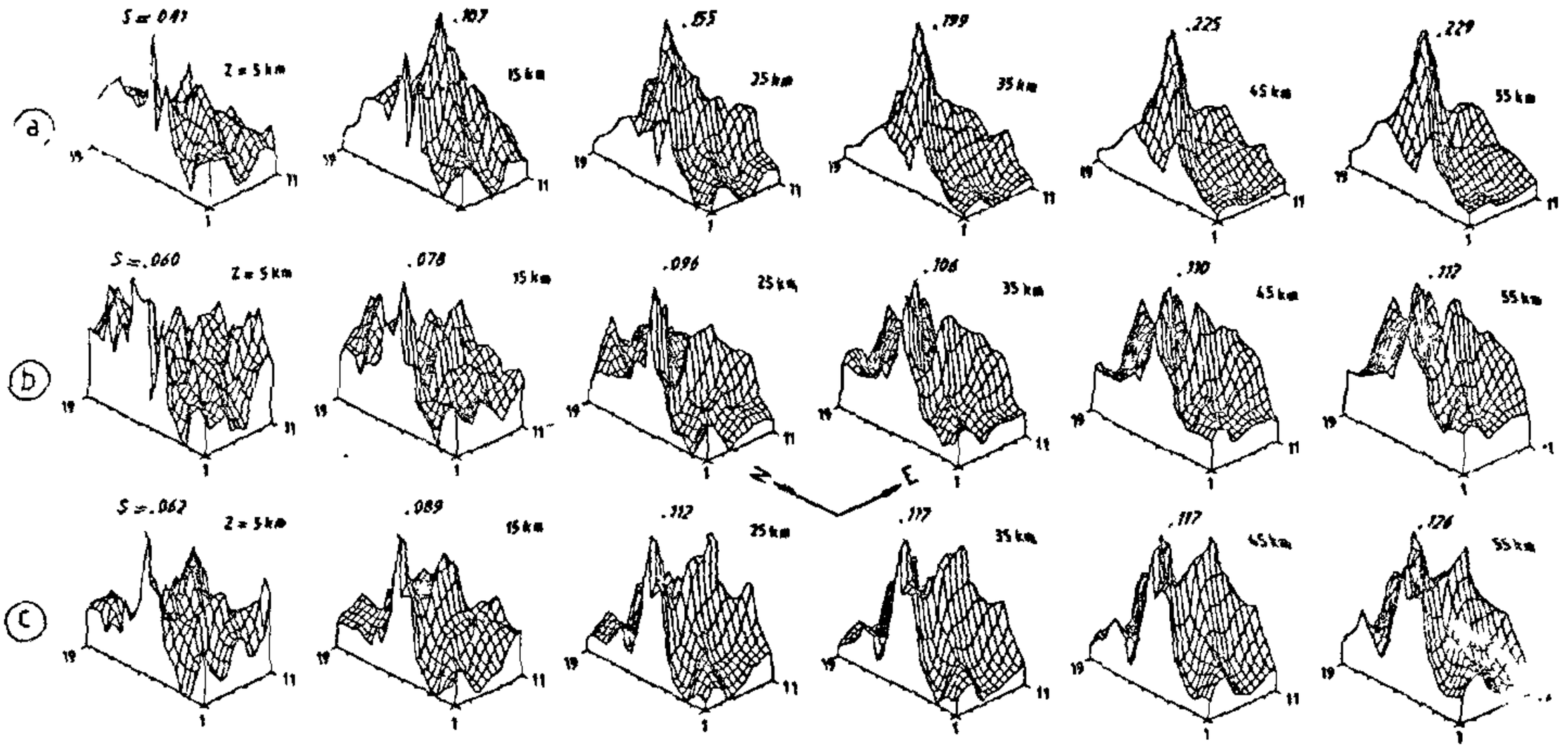

FIGURE 12(a–c) Source effect filtered semblance plot for event averaged over the azimuth range 340–350° (figure 6a), 45–65° (figure 6b) and 100–115° (figure 6c). Grid specifications as in figure 10.

The two parameters of anisotropy obtained from splitting measurements are the direction of fast velocity 'α', measured clockwise from north and 'δt' the delay time between the two quasi shear phases due to anisotropy.

The validity and applicability of this technique to data from WWSSN (World Wide Standard Seismic Network) is demonstrated by us for the first time thereby making it possible to map continental anisotropy with a large database distributed globally. By this, we have demonstrated the hidden potential of a large unexploited 3-component data that contains vital information about the palaeo and present deformations, convective history of the mantle, present day plate motion displacement and various other geodynamic processes that left their imprints on the continental lithosphere. The first report of Indian continental anisotropy together with tomographic models thus prove to be very effective in providing valuable constraints on the evolution of various geotectonic units of the south Indian shield.

The nature of seismic anisotropy in the crust/mantle beneath the Deccan volcanic province (DVP) and peninsular gneiss of India is investigated with a view to study lithospheric deformation, if any, that may be associated with source of Deccan basalts or typical with shields. Continental anisotropy results at Poona (POO) and Hyderabad (HYB) inferred from shear-wave splitting measurements and at other south Indian stations based on teleseismic time-term analysis are presented. The fast velocity directions obtained at HYB (N 20° E) and POO (N–S) are also reflected as the fast azimuth direction (NNE–NE) from time-term analysis. This analysis reveals a coherent NNE–NE fast axis trend at all the south Indian stations including POO (figure 13).

The near similar fast velocity directions at POO and HYB together with the presence of deep continental roots provide valuable constraints on the source region of the Deccan basalts. These evidences point towards the presence of the same unperturbed upper mantle

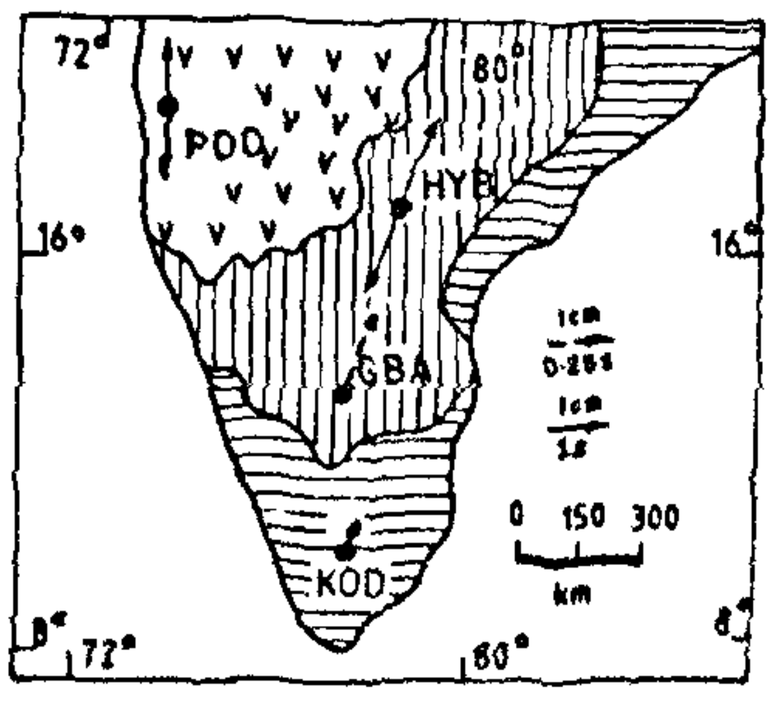

FIGURE 13 Fast velocity axis direction in south Indian shield based on shear-wave splitting and time-term analysis.

configuration beneath the Precambrian peninsular gneiss (*HYB*) and the *DVP (POO)*.

CONCLUSION

Southern Indian shield is a living geological dictionary. The exploration of this complex geological horizon is a fascination, challenge and dream to a student of tectonics. The results presented here are in no way complete. The research initiative is only an honest attempt to add some more knowledge (or "confusions") to the existing ones. It is infact a voyage to infinity within a finite framework. The ultimate goal, however, remains to discover an order in this chaotic world.

REFERENCES

1. Naqvi, S. M. and Rogers, J. J. W., *Precambrian Geology of India*, Oxford Press, New York, 1987, p. 223.
2. Herrin, E., Seismological tables for P. *Bull. Seismol. Soc. Am.*, 1968a, 58, 1196–1219.
3. Herrin, E., P-wave velocity distribution in mantle. *Bull. Seismol. Soc. Am.*, 1968b, 58, 1223–1225.
4. Aki, K., Christofferson, A. and Husebye, E. S., Determination of the 3-D seismic structure of the lithosphere, *J. Geophys. Res.*, 1977, 82, 277–296.
5. Ellsworth, W. L., Three-dimensional structure of crust and mantle beneath the island of Hawaii. Ph D. thesis, M.I.T. Cambridge, 1977, p. 237.
6. Taylor, S. R. and Toksoz, M. N., Three-dimensional crust and upper mantle structure of the northeastern United States. *J. Geophys. Res.*, 1979, 84, 7627–7644.
7. Hirahara, K., Three-dimensional seismic structure beneath southwest Japan; The subducting Phillipine seaplate. *Tectonophysics*, 1981, 79, 1–44.
8. Iyer, H. M., Seismic tomography. in *Encyclopaedia of Geophysics, (ed. James, D.) Nostrand Reinhold and Co., 1988.*
9. Husebye, E. S., Hovland, J., Christofferson, A., Astrom, K., Slunga, R. and Lund, C. E., Tomographic mapping of the lithosphere and asthenosphere beneath southern Scandinavia and adjacent areas. *Tectonophysics*, 1986, 128, 229–250.
10. Kaila, K. L. *et al.*, Crustal structure along Kavali–Udipi profile in the Indian Peninsular shield from deep seismic sounding. *J. Geol Soc. India, 1979, 20, 307–333.*
11. Jordan, T. H., The continental tectosphere. *Rev. Geophys. Space Phys.*, 1975, 13, 1–12.
12. Hoffman, P. F., Geological constraints on the origin of mantle *root beneath the Canadian shield. Phil. Trans. R. Soc. London*, 1990, A331, 523–532.
13. Iyer, H. M. and Healy, J. H., Teleseismic residuals at LASA-USGS extended array and their interpretation in terms of crust and upper mantle structure. *J. Geophys. Res.*, 1972, 77, 1503–1527.
14. Aki, K. and Chouet, B. Origin of coda waves: source, attenuation and scattering effects. *J. Geophys. Res.*, 1975, 80, 3322–3342.
15. Herraiz, M., and Espinosa, A. F., Coda waves. *Pageoph.*, 1987, 125, 499–577.
16. Aki, K., *Analysis of seismic coda of local earthquakes as scattered waves J. Geophys. Res.*, 1969, 74, 615–631.
17. Wu, R. S. and Aki, K., Introduction. Seismic wave scattering in three dimensional heterogeneous earth. *Pageoph.*, 1988, 128, 1–6.
18. Lay, T., Analysis of near source contributions to early P-coda for underground explosion. *III. Inversion for isotropic scatterers.* Bull. Seismol. Soc. *Am*, 1987, 77, 1767–1783.
19. Nikolaev, A. V. and Troitsky, P. A., Lithospheric studies based on array analysis of P-coda and microseisms. *Tectonophysics*, 1987, 140, 103–1113.
20. Dewey, J. R. and Burke, K. C. A., Tibetan, Varsican and *Precambian basement reactivation: Product of Continental* collision. *J. Geol.*, 1973, 81, 683–692.
21. Swaminath, J., Ramakrishna, M. and Vishwanatha, M. N., Dharwar stratigraphic models and Karnataka craton evolution, *Rec. Geol. Surv. India, 1976, 107, 149–175.*
22. Arora, S. K., A study of the earth's crust near Gauribidanur, South India. *Bull. Seismol. Soc. Am.*, 1971, 61, 671–683.
23. Berteussen, K. A., Husebye, E. S., Mereu, R. F. and Ram, A., Quantitative assessment of the crust-mantle heterogeneities beneath the Gauribidanur seismic array in south India. *Earth Planet. Sci. Lett.*, 1977, 37, 326–332.
24. Chernov, L. A. *Wave Propagation in Random Medium*, McGraw Hill, New York, 1960.
25. Kennett, B. L. N., Observational and theoretical constraints on crustal and upper mantle heterogeneity. *Phys. Earth Planet. Inter.*, 1987, 47, 319–322.
26. Neidell, N. and Taner, M., Semblence and other coherency measures for multichannel data. *Geophysics*, 1971, 36, 482–497.
27. Lynnes, C. S. and Lay, T., *Inversion of P coda for isotropic* scatterer at the Yucca flat test site. *Bull. Seismol. Soc. Am.*, 1989, 79, 790–804.
28. Lacoss, R. T., Review of some techniques for array processing, in *Exploitation of Seismograph Networks*, (ed. Beauchamp, K. G.) Noordhoff International Publishing, Leiden, The Netherland, 1975, pp. 11–24.
29. McCarthy, S. A., Powell C. A. and Rogers, J. J. W., A relative residual study of the southern peninsula of India using Gauribidanur seismic array, in *Precambrian of South India*, eds. Naqvi, S. M and Rogers, J. J. W. *Geol. Soc. India*, Bangalore. 1983, 525–552.
30. Kind R., Kosarev, G. L., Makeyeva, L. I. and Vinnik, L., *Observation of laterally inhomogeneous anisotropy in the* continental lithosphere. *Nature*, 1985, 318, 358–361.

ACKNOWLEDGEMENTS: We were tuned to the rhythm of Teleseismic Tomography by Dr. H. M. Iyer. No word is enough to express our gratitude for his kind advice and well wishes. The operational support for seismological stations came from several national organisations/Universities. We are thankful to all of them.